Metrology Advancements towards Diffraction-Limited X-ray Optics

Mallory M. Whalen^a, Sarah N. T. Heine^b, Alan Garner^b, Brandon D. Chalifoux^c, Herman L. Marshall^b, Ralf K. Heilmann^b, and Mark L. Schattenburg^b

^aDepartment of Mechanical Engineering, Massachusetts Institute of Technology, Cambridge, MA, USA

^bKavli Institute for Astrophysics and Space Research, Massachusetts Institute of Technology, Cambridge, MA, USA

^cJames C. Wyant College of Optical Sciences, University of Arizona, Tucson, AZ, USA

ABSTRACT

Next-generation X-ray telescopes require mirrors with surface height errors of a few nanometers. Traditional Fizeau interferometry is limited due to the characterization of reference surfaces. Axial shift mapping (ASM) is a self-referencing interferometric method that can separate the reference surface from the surface under test. This paper discusses the necessary measurement uncertainty for the Lynx X-ray Observatory concept as well as potential diffraction-limited telescopes. Plans to verify the accuracy of ASM with at-wavelength measurements are discussed.

Keywords: X-ray optics, shear interferometry, at-wavelength metrology, grazing-incidence mirrors

1. INTRODUCTION

Next-generation X-ray observatories, such as the Lynx X-ray Observatory concept, require well-figured and lightweight optics to achieve the angular resolution and sensitivity required to study supermassive black hole growth, map hot gas around galaxies and in the Cosmic Web, and investigate high-energy processes related to stellar evolution and ecosystems.¹ In a departure from the thick, full-shell optics used for the Chandra X-ray Observatory, the Lynx Concept utilizes the silicon meta-shell optics technology which requires around 40,000 silicon mirror segments, around 100 mm by 100 mm in length and width and less than 1 mm thick. Lynx requires an overall angular resolution of 0.5 arcsecond half-power diameter (HPD) with each mirror pair, comprised of a primary and secondary mirror with a Wolter–Schwarzschild prescription, achieving better than 0.2 arcsec HPD.² The figure accuracy of these mirrors must be only a few nanometers root mean-square (RMS). The Wolter prescription is a highly-off axis conic. Fizeau interferometry is the most suitable metrology method to fabricate and characterize segmented X-ray mirrors, as it is mature and scalable for high-volume manufacturing. However, Fizeau interferometry is limited by the quality of the reference and null surfaces that the surface under test (SUT) is compared to.

To overcome the limitations created by the quality of the reference surfaces, we have previously introduced Axial Shift Mapping (ASM), a self-referencing interferometry technique for near-cylindrical mirrors where the SUT is shifted between measurements.³ ASM was first performed at the University of Arizona and the setup has now been transferred to the Space Nanotechnology Lab at MIT. Figure 1 shows the experimental setup and coordinate frame. The cylindrical wavefront is created by a computer generated hologram (CGH). Two planar mirrors, called known artifact mirrors (KAMs), measure two rigid body rotations, e_{θ_x} and e_{θ_z} , during shifting so that the absolute axial figure of the SUT and reference can be unambiguously separated. ASM alone gives the profile along each axial trace of the mirror. Their tilt about x, or the local axial slope, is unknown. Adding in a lateral shift, realized as a small rotation about y, extracts the axial slope of each axial trace.⁴ Section 3 compares the U of A ASM results to those obtained at MIT.

Further author information: (Send correspondence to M.M.W.)

E-mail: malw at mit.edu

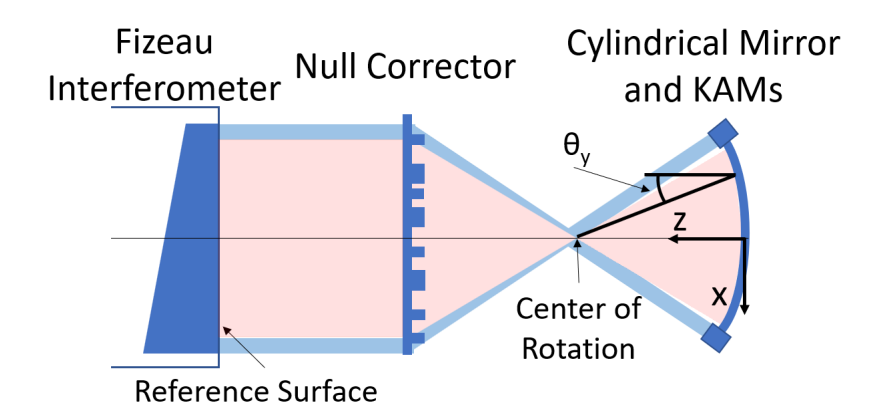


Figure 1. Fizeau interferometry setup for Axial Shift Mapping. A computer generated hologram acts as the null corrector for the cylindrical mirror. Two planar mirrors, called known artifact mirrors (KAMs), are characterized using a three-flat test and are used to measure rigid body errors in e_{θ_x} and e_{θ_z} during shifting. The cylindrical wavefront is shown in red and the collimated wavefronts for the KAMs are shown in blue.

Surface height measurements obtained with Fizeau interferometry can be used to guide the figuring of X-ray mirrors. Ion beam figuring (IBF), a deterministic polishing process, is used for the final figure correction of mirrors. The dwell-time, and thus the volumetric removal, at each mirror location during IBF is determined from surface height metrology of mirror segments. After final figuring, the overall performance of a mirror is most accurately verified by at-wavelength measurements in an X-ray beamline. Focal spot measurements before and after figuring can be used to verify the accuracy of Fizeau metrology. Section 4 discusses plans for at-wavelength metrology at MIT to provide validation of our Fizeau metrology methods.

2. METROLOGY REQUIREMENTS FOR FUTURE X-RAY OPTICS

The current state of the art technology for high-resolution, segmented X-ray optics for astronomical applications has been developed at the Next Generation X-ray Optics (NGXO) group at NASA Goddard Space Flight Center (GSFC). The NGXO manufacturing process for silicon segmented optics has demonstrated a 0.5 arcsec HPD (two reflection equivalent) mirror with a 5 nm height error after removal of sagittal depth.² The NGXO uses IBF for final figure correction of their mirrors. The NGXO group states that the final mirror quality is metrology limited; their Fizeau metrology of the individual mirror segments limits the ability of IBF to correct figure errors.⁵ IBF can only correct spatial wavelengths larger than the diameter of the ion beam. NGXO mirrors have been figured with a 9 mm ion beam.⁶ IBF beam diameters can go down to 0.5 mm.⁷ Figure 2 shows the power spectral density (PSD) of an NGXO mirror compared to a mirror from *Chandra*. The NGXO and *Chandra* PSD data are taken from Riveros et al.⁵ The NGXO data shows a beam break diameter around 10 mm, presumably figured on NGXO's IBF machine, as well as the presumed limits from metrology at low spatial frequencies. The yellow NGXO+ line shows the potential PSD improvements with better metrology. The purple NGXO+ line shows the potential PSD improvements with better metrology and a smaller ion beam diameter.

Understanding the 0.2 arcsec HPD requirement in terms of surface height metrology can be done by assuming the errors on the mirror are sinusoidal in nature. Additionally, as interferometers are most suitable for measuring low spatial frequency errors and IBF can only correct spatial wavelengths larger than the ion beam diameter, a ray tracing-based approximation can be used. The transition from low-spatial frequency to mid-spatial frequency for segmented X-ray optics occurs around spatial wavelengths shorter than 10 mm. Figure, or low spatial frequency errors, are responsible for broadening the core of the point spread function (PSF). A slope error, θ , will deviate the ray by 2θ if the error is axial, while an azimuthal slope error will deviate the ray by $\theta \tan(2\alpha)$, where α is the graze angle. Thus, axial slope errors in the low-spatial frequency regime are the dominant cause of PSF broadening. Assume the axial errors take the form of $z = A\sin(2\pi y/\Lambda)$, where A is the amplitude, Λ is the spatial wavelength, z is the surface height, and y is the axial coordinate on the mirror. The RMS height is $A/\sqrt{2}$ and the RMS slope is $2\pi A/(\sqrt{2}\Lambda)$. The HPD from a Gaussian distribution of slope error from two mirrors with uncorrelated errors is 3.84 times the RMS slope. For a desired 0.2 arcsec HPD, the RMS height for wavelengths

from 10-100 mm would need to be 0.4-4 nm, respectively. The measurement uncertainty of these errors needs to be less than the desired error, indicating that Fizeau metrology for X-ray mirrors needs single to sub-nanometer measurement repeatability for longer spatial-wavelengths, with even stricter requirements near the mid-spatial frequency transition.

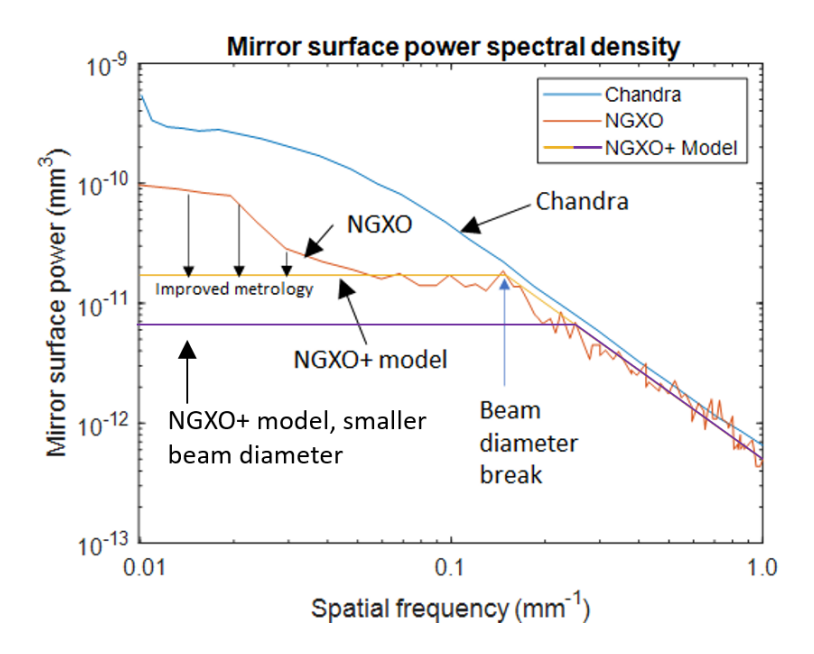


Figure 2. Power spectral density (PSD) of NGXO and *Chandra* mirrors as well as anticipated improvements of the NGXO mirrors with better metrology and reduced ion beam diameter. The NGXO and *Chandra* PSD data are taken from Riveros et al.⁵

What would the requirements look like for a telescope with even greater resolution, such as in the diffraction-limited design presented by Chalifoux et al.¹¹? The Maréchal criterion can be used to determine the diffraction-limited wavefront quality. The criterion states that wavefront errors need to be less than $\lambda/14$ RMS, where λ is the optical wavelength. RMS wavefront is equal to $2\sqrt{2}\sin{(\alpha)}RMS_{surface}$.¹² The $2\sqrt{2}$ accounts for two mirror reflections off of mirrors with uncorrelated errors. The $\sin{\alpha}$ accounts for the foreshortening of errors at graze angle α . For $\lambda=1$ nm and $\alpha=1^{\circ}$, a diffraction limited wavefront would require a surface RMS of less than 1.5 nm. This is not unimaginable; Kirkpatrick-Baez mirrors for hard X-ray have been figured to 0.1 nm RMS surface quality using forms of stitching interferometry.¹³ For a given PSD of a mirror surface, the surface RMS is the square root of the PSD integrated over the entire frequency range. If the PSD of an X-ray mirror takes the form of the NGXO+ model shown in Figure 2, an ion beam diameter of 3 mm would produce a surface RMS of less than 1.5 nm and create a diffraction-limited mirror (assuming appropriately capable metrology for IBF dwell-map creation).

3. ASM SETUP AT MIT

The ASM setup has been transferred from the University of Arizona to MIT. Detailed information about the experiment and mathematical derivation of the rigid body error removal and surface extraction can be found in Wisniewski et al.³ Figure 3 shows the fundamentals of ASM. Figure 4 shows the experimental setup at MIT.

An identical test to the test performed at the U of A was done at MIT. The U of A achieved a 4.4 nm RMS repeatability for both the extracted reference and test surface along the axial direction. MIT obtained a comparable 4.3 nm RMS repeatability for the extracted test surface and a 4.1 nm RMS repeatability for the extracted reference surface. Figure 5 shows the extracted surface under test and Figure 6 shows the extracted reference surface each averaged over 5 measurement campaigns at MIT. Table 1 details the repeatability of individual measurement campaigns performed at MIT. The RMS of the difference between each campaign and

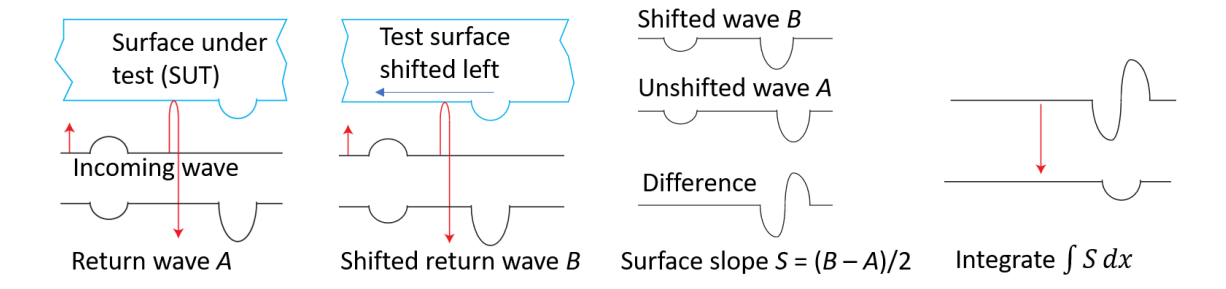


Figure 3. Pictographic description of ASM. The difference of the shifted and unshifted waves creates a map of the test surface slope where the static reference error cancels out. Integration of the slope map yields a surface map. Both the reference and test surfaces can be obtained by a least mean squares method.

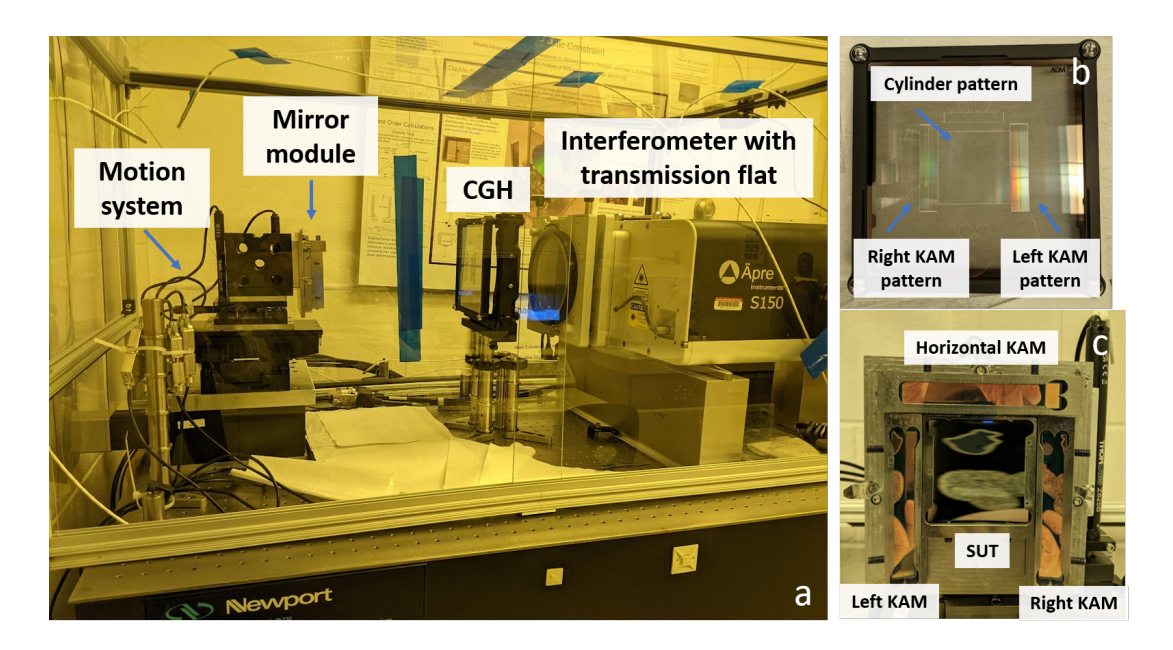


Figure 4. (a) ASM setup at MIT showing the mirror module on the 6 degree of freedom motion stage, the CGH, and the interferometer. (b) CGH with left and right KAM patterns and cylinder patterns labeled. (c) Close-up of mirror module with left and right KAMs, cylinder SUT, and horizontal KAM installed. The horizontal KAM is not utilized for ASM.

the mean measurement of the 5 campaigns was taken as the repeatability. Each measurement campaign consists of 10 shifting measurements. Each shifting measurement is comprised of 20 shifts that are separated axially by 1 pixel each. During measurement, the rigid body error pitch e_{θ_x} was corrected within a tolerance of 1.5 μ rad during shifting. The remaining e_{θ_x} and e_{θ_z} rigid body errors are removed mathematically from the measurements.

3.1 Future Work for ASM

The overall goal for ASM is to provide a surface map for ion beam figuring of a mirror. The accuracy of the measurement will be evaluated by at-wavelength metrology of the mirror before and after figuring. A rotated ellipsoid test mirror has been procured for at-wavelength measurements. The prescription allows for focusing in two dimensions to create a focal spot. First, ASM will be expanded to measure the local axial slope of the mirror by incorporating lateral shifting. Additionally, the factors that affect repeatability, such as temperature variation, vibration, and retrace error, will be studied to improve the repeatability of ASM. The improved ASM technique will be used to measure the rotated ellipsoid test mirror. Comparison of the predicted focal spot from

ASM measurement to the actual focal spot size, as well as comparison to at-wavelength measurements of surface slope, will indicate the accuracy of the technique.

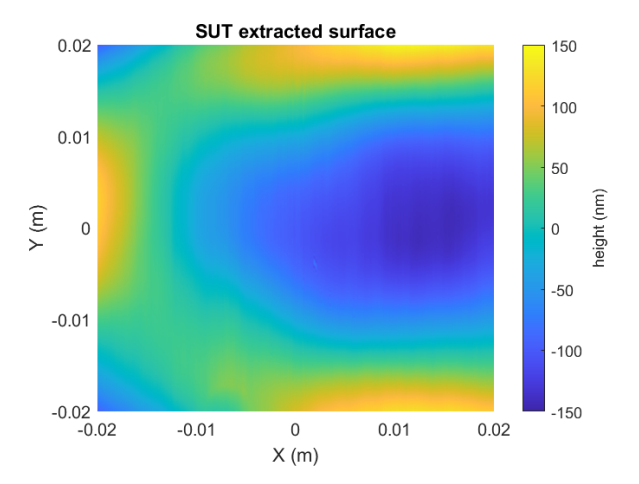


Figure 5. Average extracted surface under test from five measurement campaigns of ASM. The repeatability is 4.3 nm RMS. The circular artifact, caused by removal of an interferometer reflection issue and seen more clearly in the extracted reference surface, can be just made out near the bottom left of the extracted surface.

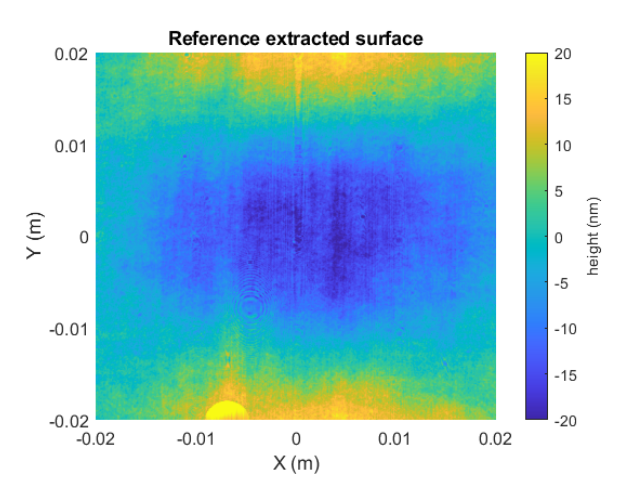


Figure 6. Average extracted reference surface from five measurement campaigns of ASM. The repeatability is 4.1 nm RMS. The circular artifact near the bottom left is caused by a data mask in that region that removes a spurious feature caused by an internal reflection issue in the interferometer.

Table 1. Repeatability of the surface under test and reference surface.

Campaign	SUT Repeatability (nm RMS)	Reference Repeatability (nm RMS)
1	2.0	2.4
2	2.4	4.4
3	4.7	3.3
4	5.2	6.4
5	7.4	4.1
Mean	4.3	4.1

4. AT-WAVELENGTH METROLOGY

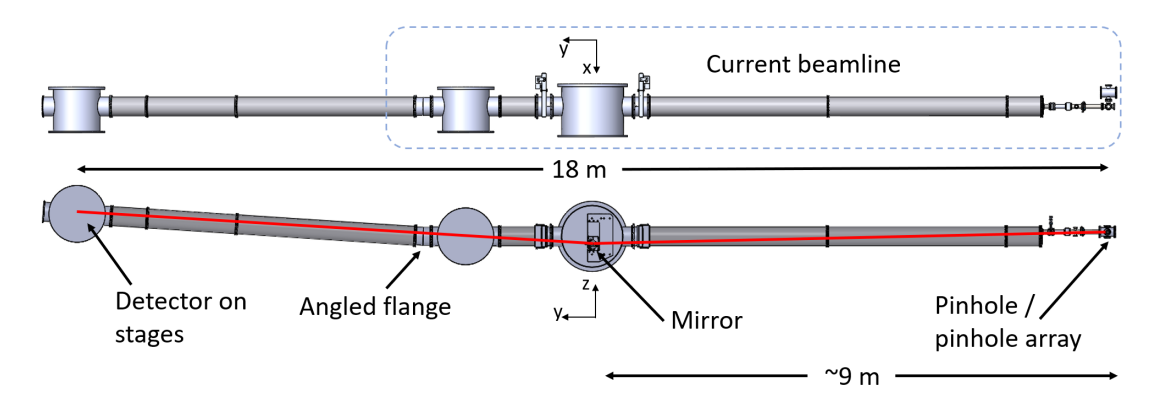


Figure 7. Proposed changes to the polarimetry beamline at MIT. The beamline will be extended and another chamber will be added to accommodate testing of X-ray mirrors with a \sim 9 m focal length. The beamline uses a Manson Model 5 source. A multilayer mirror monochromatizes the source.

The MIT polarimetry beamline is being adapted to allow for testing of ~ 9 m focal length X-ray mirrors. Figure 7 shows the current beamline as well as planned changes. The beamline will be expanded and an additional chamber will be added. The additional chamber will house an in-vacuum CMOS camera as well as a grating for lateral shear interferometry (LSI). LSI has been demonstrated to have a 0.19 nm RMS measurement error for use in characterizing extreme ultraviolet optics. ¹⁴ LSI has also been implemented for soft X-ray wavelengths. ¹⁵ Figure 8 shows the basic layout of LSI. LSI uses a grating to create sheared orders that interfere with each other. The wavefront slope can be extracted from the interference pattern.

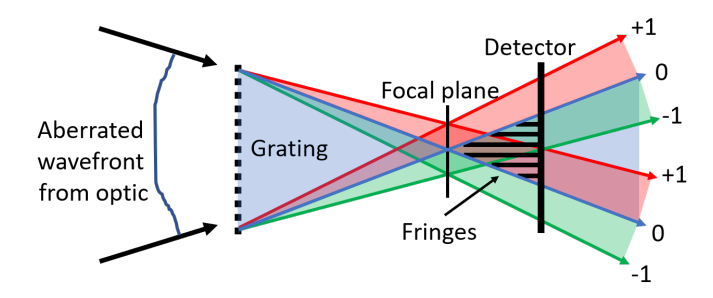


Figure 8. One possible realization of lateral shear interferometry (LSI) for at-wavelength metrology of X-ray mirrors. The grating can be placed before or after the mirror focus. The detector is placed in a Talbot plane. A high contrast self-image of the grating is created by interference of the diffracted orders. ¹⁵ LSI can be used to help with mirror alignment as well as measure wavefront slope.

5. CONCLUSION

The reduction of measurement uncertainty in Fizeau interferometry is needed for the technique to guide ion beam figuring of X-ray telescope mirrors to acceptable quality for future missions such as Lynx. Axial shift mapping removes the uncertainty caused by insufficiently characterized reference optics. The MIT polarimetry beamline is being upgraded to accommodate X-ray mirror testing. At-wavelength measurements will be compared to ASM measurements to verify the accuracy of the ASM technique.

ACKNOWLEDGMENTS

This work is funded by NASA Grants 80NSSC20K0907 and 80NSSC24K0366.

REFERENCES

- [1] Gaskin, J. A., Swartz, D., Vikhlinin, A. A., Özel, F., Gelmis, K. E. E., Arenberg, J. W., Bandler, S. R., Bautz, M. W., Civitani, M. M., Dominguez, A., Eckart, M. E., Falcone, A. D., Figueroa-Feliciano, E., Freeman, M. D., Günther, H. M., Jr, K. A. H., Heilmann, R. K., Kilaru, K., Kraft, R. P., McCarley, K. S., McEntaffer, R. L., Pareschi, G., Purcell, W. R., Reid, P. B., Schattenburg, M. L., Schwartz, D. A., Sr, E. D. S., Tananbaum, H. D., Tremblay, G. R., Zhang, W. W., and Zuhone, J. A., "Lynx X-Ray Observatory: an overview," Journal of Astronomical Telescopes, Instruments, and Systems 5, 021001 (May 2019).
- [2] Zhang, W. W., Allgood, K. D., Biskach, M., Chan, K.-W., Hlinka, M., Kearney, J. D., Mazzarella, J. R., McClelland, R. S., Numata, A., Riveros, R. E., Saha, T. T., and Solly, P. M., "High-resolution, lightweight, and low-cost x-ray optics for the Lynx observatory," *Journal of Astronomical Telescopes, Instruments, and Systems* 5, 021012 (Apr. 2019).
- [3] Wisniewski, H. J., Heilmann, R. K., Schattenburg, M. L., and Chalifoux, B. D., "Axial shift mapping: a self-referencing test for measuring the axial figure of near-cylindrical surfaces," *Applied Optics* 62, 9307–9316 (Dec. 2023).
- [4] Chalifoux, B. D., Wisniewski, H. J., Schattenburg, M. L., Heilmann, R. K., Arnold, I. J., and Whalen, M. M., "Rigid body motion tracking in axial shift mapping for measuring astronomical x-ray mirror figure," in [Optics and Photonics for Advanced Dimensional Metrology III], 12997, 157–163, SPIE (June 2024).
- [5] Riveros, R. E., Allgood, K. D., Biskach, M. P., DeVita, T. A., Hlinka, M., Kearney, J. D., Numata, A., and Zhang, W. W., "Fabrication of lightweight silicon x-ray mirrors," in [Space Telescopes and Instrumentation 2022: Ultraviolet to Gamma Ray], 12181, 222–229, SPIE (Aug. 2022).
- [6] Ghigo, M., Basso, S., Civitani, M., Gilli, R., Pareschi, G., Salmaso, B., Vecchi, G., and Zhang, W. W., "Final correction by Ion Beam Figuring of thin shells for X-ray telescopes," in [Advances in Optical and Mechanical Technologies for Telescopes and Instrumentation III], 10706, 1043–1050, SPIE (July 2018).
- [7] Schaefer, D., "Basics of ion beam figuring and challenges for real optics treatment," in [Fifth European Seminar on Precision Optics Manufacturing], 10829, 38–45, SPIE (Aug. 2018).
- [8] Harvey, J. E., "The surface PSD and image degradation due to mid-spatial-frequency errors," in [Tribute to James C. Wyant: The Extraordinaire in Optical Metrology and Optics Education], 11813, 160–173, SPIE (Sept. 2021).
- [9] Spiga, D. and Raimondi, L., "X-ray optical systems: from metrology to Point Spread Function," in [Advances in Computational Methods for X-Ray Optics III], 9209, 98–113, SPIE (Sept. 2014).
- [10] Podgorski, W. A., Bookbinder, J., Content, D. A., Davis, W. N., Freeman, M. D., Hair, J. H., Owens, S. M., Petre, R., Reid, P., Saha, T. T., Stewart, J. W., and Zhang, W. W., "Constellation-X spectroscopy x-ray telescope optical assembly pathfinder image error budget and performance prediction," in [Optics for EUV, X-Ray, and Gamma-Ray Astronomy], 5168, 318–333, SPIE (Jan. 2004).
- [11] Chalifoux, B. D., Heilmann, R. K., Marshall, H. L., and Schattenburg, M. L., "Optical design of diffraction-limited x-ray telescopes," *Applied Optics* **59**, 4901–4914 (June 2020).
- [12] Harvey, J. E., Moran, E. C., and Zmek, W. P., "Transfer function characterization of grazing incidence optical systems," *Applied Optics* 27, 1527–1533 (Apr. 1988).
- [13] Mimura, H., Matsuyama, S., Yumoto, H., Hara, H., Yamamura, K., Sano, Y., Shibahara, M., Endo, K., Mori, Y., Nishino, Y., Tamasaku, K., Yabashi, M., Ishikawa, T., and Yamauchi, K., "Hard X-ray Diffraction-Limited Nanofocusing with Kirkpatrick-Baez Mirrors," *Japanese Journal of Applied Physics* 44, L539 (Apr. 2005). Publisher: IOP Publishing.
- [14] Naulleau, P. P., Goldberg, K. A., and Bokor, J., "Extreme ultraviolet carrier-frequency shearing interferometry of a lithographic four-mirror optical system," *Journal of Vacuum Science & Technology B: Microelectronics and Nanometer Structures Processing, Measurement, and Phenomena* 18, 2939–2943 (Nov. 2000).
- [15] Goldberg, K. A., Wojdyla, A., and Bryant, D., "Binary Amplitude Reflection Gratings for X-ray Shearing and Hartmann Wavefront Sensors," Sensors 21, 536 (Jan. 2021). Number: 2 Publisher: Multidisciplinary Digital Publishing Institute.